

Author version: Meteor. Planet. Sci., vol.45(6); 2010; 990-1006

Changes in abundance and nature of micro-impact craters on the surfaces of Australasian microtektites with distance from the proposed source crater location

M. Shyam Prasad*

National Institute of Oceanography (Council of Scientific and Industrial Research), Dona Paula,
Goa – 403004, INDIA

*Corresponding author. E-mail : shyam@nio.org

Phone : 91-832-2450261; Fax : 91 – 832 – 2450602

Sandip Kumar Roy

Dept. of Geology and Geophysics, Indian Institute of Technology, Kharagpur, West Bengal,
INDIA

Avinash Gupta

Department of Earth Sciences, Indian Institute of Technology, Roorkee - 247667 Uttarakhand
–,INDIA.

ABSTRACT

Over 4600 Australasian microtektites from 11 sediment cores along a N-S transect in the Central Indian Ocean have been investigated optically for micro-impact features on their surfaces. Detailed SEM examination of 68 microtektites along this transect shows 4091 such features. These samples are located between approximate distances of 3900-5000 km from the suggested impact site in Indochina and therefore constitute distal ejecta. The morphology of the micro-impacts seems to show distinct variations with distance from the source crater. The total number of micro-craters on each microtektite decreases drastically from North to South indicating systematic decrease in the spatial density of the ejecta, and decrease in collisional activity between microtektites with distance from the proposed source crater location. Closer to the proposed source crater location, the micro-craters are predominantly small (few μm), pit-bearing with radial and concentric cracks, suggestive of violent interparticle collisions. The scenario is reverse farther from the source crater with smaller numbers of impacted microtektites due to increased dispersion of the ejecta and the micro-craters are large and shallow, implying gentle collisions with larger particles. These observations provide systematic ground truth for the processes that take place as the ejecta of a large oblique impact which generated the Australasian tektite strewn field is emplaced. The micro-impacts appear to take place during the descent of the ejecta and their intensity and number density decrease as a function of the spatial density of the ejecta at any given place and with distance from the source region. These features could help understand processes that take place during ejecta emplacement on planets with substantial atmosphere such as Mars and Venus.

Key words : meteorite impacts, tektites, microtektites, microimpacts, Mars, Venus, ejecta.

INTRODUCTION

There are > 170 known impacts on the earth (Earth Impact Database, <http://www.unb.ca/passc/ImpactDatabase>), but only 4 tektite strewn fields are known. Tektites are glassy impact ejecta distributed over large regions called strewn fields. Four tektite strewn fields of Cenozoic age are known, of which the youngest, the Australasian tektite strewn field is perhaps the largest, spread over 50 million km² of the surface of the earth (Glass et al., 1979; Glass and Koeberl 2006). Although the craters that produced the other three tektite strewn fields (North American, East European, Ivory Coast strewn fields) have more or less circular shapes, because the distribution of ejecta is more sensitive to angle of impact (Pierazzo and Melosh 2000), the non-centrosymmetric nature of tektite strewn fields suggests oblique impact angles. The path-breaking oblique impact simulation experiments of Gault and Wedekind (1978) have improved our understanding of the cratering process manifold. Subsequently, several studies have been undertaken to understand oblique impacts because, on planetary surfaces, they are normal (Schultz 1996; Schultz 1999; Pierazzo and Melosh 2000a; 2000b). Some recent investigations have specifically modeled tektite-producing impacts (Stoffler et al. 2002; Artemieva 2002). All these and related studies have been able to address various aspects of meteorite impact such as melt production, ejecta distribution, effects of atmospheric interactions.

Tektite and especially micro-tektite strewn fields come with an inherent advantage of being distributed over vast geographic areas as demonstrated in three of the four strewn fields (Koeberl 1994; Glass 1990). Microtektites belonging to the Australasian tektite strewn field have been found in 75 locations so far (Prasad et al. 2007). The advantage of a large geographic distribution is that systematic effects of radial range from the parent crater can be investigated. This is especially true for a young impact event such as the Australasian impact event (0.77 Ma age : Kunz et al. 1995), where normal sampling techniques are sufficient for recovering well preserved ejecta from the ocean floors. Thus, large numbers of sediment cores containing Australasian microtektites can be used to define the outer limits of the strewn field (Glass et al. 1979; Glass and Wu 1993). The distal ejecta in the form of microtektites and shock metamorphosed rock and mineral grains decrease in size and abundance from Indochina up to a geographic distance of over 6000 km (Glass and Pizzuto 1994; Glass and

Koeberl 2006; Prasad et al. 2007). This particular aspect of ejecta distribution has been used in the present study.

The Australasian microtektites contain micro-impact features on their surfaces which have provided evidence for processes that take place as distal ejecta re-enters the atmosphere (Prasad and Sudhakar 1996; 1998; Prasad and Khedekar 2003). In this study we have examined surface features on 4604 Australasian microtektites ranging from 180 to 1530 μm diameter, in 11 sediment cores along a N-S transect stretching over 1300 km in the Central Indian Ocean. These samples are located in a radial range of 3899 to 5162 km from the postulated impact site in Indochina (18°N ; 104°E : Prasad et al. 2007). We record the systematic variation in the morphology of the microimpact-craters from North to South along this transect and interpret these variations in terms of the processes that took place after solidification of the microtektites. The aim of the present study is to characterize the processes that take place between ejecta particles with increasing radial range from the source crater.

MATERIALS AND METHODS

The samples investigated in this study have been collected during several cruises to the Central Indian Ocean between 1993-2003. Australasian microtektites from 11 sediment cores have been examined for this study, from which 4604 microtektites dominantly $>250\ \mu\text{m}$ diameter were extracted and investigated for impact generated, small scale surface features, however in two of the northernmost samples AAS 38/1 (3899 km) and in AAS 38/2 (4174 km) we also observed microtektites of $<250\ \mu\text{m}$ diameter. It may be noted here : the number of km given in the parenthesis accompanying sample numbers throughout the text are the radial distances from the source crater suggested by Prasad et al. (2007), based on microtektite abundances. Further, the impact crater responsible for the Australasian strewn field is not discovered yet, however, most investigators using several different parameters have arrived at the opinion that the crater is in the Indochina region (eg. Ma et al. 2004; Glass and Koeberl 2006). In this study, we consider the impact site predicted by Prasad et al. (2007) for indication of radial distance of the samples used here. The methods employed in isolating the

microtektites have been explained in Prasad et al. (2007). The sediment cores have been recovered from the Central Indian Ocean at different locations starting from north at $04^{\circ}58.564'S$ and $078^{\circ}01.204'E$ up to south $18^{\circ}19.480'S$ and $77^{\circ}55.737'E$ (Fig. 1). The details of the numbers of microtektites recovered at each location are given in Table 1. Sample no. AAS38/1 is the northernmost sample and AAS38/5 is the southernmost. The distance between these two samples is about 1300 km which forms the N-S transect of this study. A seafloor surface area of 3.5×3.5 cm was used in most of the sediment cores for microtektite abundance determination. In two of the southernmost samples, AAS 62/55 (5008 km) and AAS62/56 (4969 km) the rates of sedimentation are very low, spade corer having sampling capacity of $50 \text{ cm} \times 50 \text{ cm}$ was deployed here for collection of a large number of microtektites. We were therefore able to recover and observe several thousand microtektites, especially in AAS 62/56 (4969 km) by scanning a large quantity of sediment here. The microtektite abundance values given in this sample, as well as in all the samples (Table 1) are the total number of microtektites of $>125 \mu\text{m}$ diameter/ cm^2 of seafloor

The microtektites from each of the cores were observed under the binocular microscope at magnifications up to 50X for possible impact generated features. This gave us the total percentage of impacted microtektites for each sample. Etching of microtektites could pose a problem in identifying micro-craters on microtektite surfaces. The quantity of etching observed on Australasian microtektites ranges from 2 – 16 μm (Glass 1984). On smaller microtektites (125-250 μm diameter), especially, it is much more difficult to recognize micro-impact features because these microtektites in view of their size do not register larger micro-craters : projectiles that produce larger micro-crater could easily fragment them. Therefore the sizes of observable micro-impacts on their surfaces are close to the observation limit of micro-craters using the binocular microscope. At best, micro-craters having diameters of $\sim 20\mu\text{m}$ could be recognized under the binocular microscope without much ambiguity. This aspect has been described in detail earlier (Prasad and Khedekar 2003). However, the error would remain uniform for all the samples. Further, representative numbers (similar appearing microtektites) of the impacted microtektites were examined in detail in a JEOL JSM 5800 LV scanning electron microscope to identify even the smallest possible impact feature. In all, 68 microtektites from all nine cores were examined in the SEM and 380 SEM images have been obtained. All images were thoroughly observed for impact craters. Absolute number of impacts

were counted on each microtektite and their diameters were measured. However, there would still be a small region (maybe 20-30%) on each microtektite that could not be observed at all or at least not well enough to identify and document the presence of micro-impact craters, especially the smaller ones. Therefore the number of observed micro-impacts on each microtektite is probably less than the actual number present. The longest dimension is measured in case of slightly oval micro-craters. Grooved craters, which form by very low angle impacts are not considered for crater size determination in this study because of the inherent difficulty in determining the crater sizes in the highly oblique impacts (eg. Fig. 3e). However, these impacts are counted when determining number of micro-craters/microtektite. In all, 4091 impact generated features have been observed. At each site the microtektites were dominantly yellow with others being light green or brownish in color indicating that they all have roughly the same composition.

Several parameters were observed for this study : microtektite diameter, percentage of impacted microtektites, size range of microtektites, size range of micro-craters, number of micro-impacts on individual microtektites (Table 1). Size ranges of micro-impacts on individual microtektites (Table 2) and the variance in the micro-crater sizes with increasing radial distance (Table 3), total impacts/microtektite (Table 2) which gives an idea of the collisional activity in the ejecta at a given radial distance from the source. Further, we also calculated the spatial density of impact micro-craters at each of the locations. Different numbers of microtektites have been searched from each of the samples for micro-craters, in order to obtain an equilibrated number of impacts for a given area, the following procedure was adopted. Number of micro-craters per microtektite has been counted for all the samples, further, the average diameter of the microtektite has been measured for all the samples. For uniformity, the total number of micro-impacts in a given sample has been calculated to the number per average sized microtektite in a particular sample and multiplied by the percentage of impacted microtektites at each of the locations. This is effectively the spatial density of micro-impacts which is calculated as : number of micro-craters/cm² of the seafloor at a given location

Since all the above parameters relate to radial range from the impact site, they are all plotted on panels having a common X-axis of radial distance to arrive at the variations and

interrelations between these parameters with increasing radial distance from the source crater (Figs. 6, 7).

DESCRIPTION OF IMPACTED MICROTEKTITES

The character of the micro-impacts in terms of their sizes, types, and numbers on each microtektite changed systematically N-S. The micro-craters along the transect are therefore described for each sample below. The description of micro-craters follows the classification carried out earlier by Prasad and Khedekar (2003) into two major classes :

(1) Accretionary impact features : comprises of features such as projectiles that are welded to the target, disrupted projectiles - half-buried or flattened upon impact, spatter and pancakes which are projectiles splattered on target surfaces. These are caused by low-velocity collisions.

(2) Erosive/Destructive impacts : Erosive impacts include pit craters, pitless craters and oblique impacts where grooves are made by impacting projectiles having highly inclined trajectories. Fragments also represent destructive impacts.

The description of micro-craters follows that given by Hörz et al. (1971) for lunar micro-craters. Pit craters have been defined by them as craters having a central depression which have a glass-lined pit. Some of these craters had a central elevated area which contained a cup-like depression and these were described as stylus pit craters. Further, Hörz et. al. (1971) also described somewhat shallow circular craters which did not have a central glass-lined nor a stylus pit, such craters were termed pitless craters - these craters had relatively larger diameters than the 'pit' craters and they suggested that the pitless craters could either be generated by projectiles with lower impact velocities or these could even be hypervelocity impact micro-craters where the central pit has been excavated.

During selection of microtektites for SEM examination, as was done during our previous studies as well (Prasad and Sudhakar 1998; Prasad and Khedekar 2003), care was taken to observe only those microtektites which showed least characteristics of etching.

AAS 38/1 (3899 km):

Location: 04° 58.564'S & 78° 01.204'E

This is the northernmost sample. Twelve impacted microtektites from this sample have been observed under the SEM, in the size range 275-911 μm . Dominant population of the craters are of erosive type (Fig. 2), i.e., those which contain a central pit which is surrounded by radial and concentric cracks, indicative of high velocity impacts (Hörz et al., 1971). This could be misleading, as observed in our earlier studies as well (Prasad and Sudhakar 1998; Prasad and Khedekar 2003), both the hosts and the projectiles are hot at the time of their collisions; therefore, it would take much lower projectile velocities than determined by simulation on cool targets to register what seem like hypervelocity impact microcraters. In addition, the radial cracks here are not numerous as observed on cool targets (Christiansen 1993), further emphasizing the fact that the targets were in a hot condition. This aspect is common to almost all the observed samples in this study. Fragments are taken in this study as indicative of destructive impacts; they are broken microtektites, many of which contain some evidence of the impact/collision that caused fragmentation (eg. Fig. 3 b; Fig. 4 a). However, some other fragments which have conchoidal fractures and do not bear evidence of a collision, and could have resulted due to differential cooling upon contact with sea water (Glass et al., 1997). In this sample, 1.59 % of all observed ejecta here are fragments. The more erosive craters contain concentric as well as radial cracks (Fig. 2 f). In addition, there are some interesting accretionary features, resembling pancake structures (Fig. 2,d), which are caused by low velocity impacts of projectiles which are in a plastic state. These features stand out as positive features on the host microtektites (Fig. 2 d,e).

All the microtektites that were observed in the SEM (12) in this sample contain a large concentration of craters (Table 2). Six microtektites have more than 100 impacts each. Total number of impacts on the 12 microtektites observed from this sample are 1171, of which 47 are low angle oblique craters which have a groove-like depression (eg. Fig. 3e). In all cases, the spall diameter of the crater is taken for determining crater diameter. The majority of the micro-impacts are of sizes $<25 \mu\text{m}$. (Table 3; Fig. 2a,b; Fig.6). This indicates interaction within a dense swarm of very small particles at high relative velocities. This location also has

the highest spatial density of impacts, i.e., it contains 230 micro-craters/cm² of the ocean floor (Table 2).

AAS 22/8 (4052 km):

Location : 07^o 05.289'S & 78^o 07.712'

In all, 10 microtektites were studied in detail with the SEM from the 25 impacted ones observed during optical observations. This sample also contains the largest number of fragments (6.81%), some fragments contain micro-craters (Fig. 3 b). Three of the 10 chosen for SEM observation are also fragments representing destructive impacts. The other 7 impacted microtektites contain 455 impact craters of which only 2 are observed as very low angle oblique impacts. The diameters for the other 453 craters are measured. There is a large variation in the number of micro-craters observed on individual microtektite surfaces in this sample. The least number observed is 17 and the largest number of micro-craters observed on a single microtektite in this sample is 222 (Table 2). This contrasts with the sample located north of the present one (AAS38/1; 3899 km) where all the microtektites observed had large number of micro-craters on their surfaces. The spatial density of impacts here (80 micro-craters/cm²) is also less than in AAS38/1. This sample also contains dominantly small sized craters (69% are < 25 µm in diameter : Table 3, Fig.6). Craters which contain a pit as well as pitless ones were observed. Within the pit bearing class both stylus as well as glass lined pits were found. Most of the pitless craters are found to be large in size. A few accretionary features containing adhering projectiles (Fig. 3 a) and 'pancakes' are also observed in this sample.

AAS 38/2 (4174 km):

Location: 8°29.868'S & 77°59.761'E

Out of the 20 impacted microtektites found by binocular microscopic observation, 7 in the size range 647-1530 µm were chosen for SEM study. In all, 869 micro-craters were found

on these microtektites including 311 highly oblique impacts which have a groove-like feature (Fig. 3e). Therefore, crater diameters are measured only for 558 micro-impacts (circular or near circular craters) out of which 51.6% are small (<25 μm diameter); an increase in the craters having larger diameters is observed in this sample when compared with the samples to the North (Table 3; Fig. 3d, Fig. 6). The spatial density of micro-impacts ($34/\text{cm}^2$) shows a decrease when compared to samples north of this location.

While the two samples north of this location contained dominantly erosive type of impacts, the micro-impact population here is mixed with two microtektites containing high numbers of accretionary impacts, yet these microtektites also contain several erosive impacts.

A unique disc-shape microtektite in this sample has accumulated 304 impacts (Fig. 3 e), most of them are craters having groove-like features which represent a projectile with a highly oblique trajectory. The oblique craters are found on both sides of the microtektite, indicating tumbling during flight. Because of its shape, the surface offered for the projectiles is flat, which is rotating and tumbling therefore offering a target at extreme low angles to the projectiles, as discerned from the different trajectories shown by the grooves on this specimen (Fig. 3 e). Also, the large number of impacts is also indicative of ejecta having an extremely high density here.

When compared with the two samples north of this one, the impacts in the lower size category decreases (Table 3; Fig 6), and there is a slight increase in the percent of craters > 50 μm . The type of impacts show a mixed population here also with large pitless craters (eg. Fig. 3 d) and smaller craters with pits.

AAS 22/7 (4284 km):

Location: 10°00.988'S 78°08.971'E

Nine out of the 19 impacted ones found in this samples have been observed via SEM. Four out of the 9 observed are fragments (Fig. 4 a). The other 5 microtektites have recorded 293 impacts including 31 highly oblique micro-craters. Hence, the diameter is measured only for 262 craters out of which 62.97% are < 25 μm in diameter, 30.9% are

between 26-100 μm and 6.11% are large ($>100 \mu\text{m}$ diameter) craters. The spatial density of micro-craters is lower here (26 / cm^2). (Table 2).

Stylus pit craters are more dominant in this sample. In addition, that many pit only craters are also recorded as closely spaced clusters indicating sandblasting of the host. Craters are predominantly erosive by nature and only a few microtektites have projections similar to ones shown by Prasad and Khedekar (2003).

Further, on one microtektite many submicron craters are observed (Fig. 3 f). These craters bear an uncanny resemblance to the submicrometer craters on the rocks of Apollo 17(71055, 74255) (Hutcheon 1975).

The dominant micro-crater population in this sample is of the small variety ($<25 \mu\text{m}$). Micro-craters impacts in this sample and in the sample south of this one (AAS38/3; 4708 km) have similar characteristics. This sample also continues with trend of decrease in the spatial density of micro-craters.

AAS 38/3 (4708 km):

Location: 12°34.831'S 75°15.351'E

Eight impacted microtektites have been observed from this sample. In all, 609 impacts including 34 craters with groove-like shapes were observed. Accurate diameters for the remaining 575 craters were measured and subdivided into 428 (74.43%) small craters with diameters less than 25 μm , 130(22.6%) medium size craters in the diameter range 26-100 μm and 17(2.95%) large craters, $>100 \mu\text{m}$ diameter.

This sample contains one microtektite of relatively small diameter ($\sim 400 \mu\text{m}$), which has recorded the maximum number of craters (441 impacts) among all the samples observed in this study (Fig. 4 c, d). Most of the impacts on this particle are also small in size but representative of high energy as shown by glass lined pits as well as stylus pit craters formed by hypervelocity impacts. On this microtektite, there are several closely spaced clusters of high velocity craters and almost of similar sizes—implying similar size projectiles have, in a very small gap of time (considering the time taken for the ejecta to be thrown out and the time it would be mid air – few seconds to minutes), have hit this microtektite by the hundreds. The

other impacted microtektites in this sample show a range of 8 – 65 impacts/microtektite (Table 2), This disparity is perhaps indicative of the overall reduction in collisional activity in the ejecta at this distance from the source. The spatial density of micro-impacts here is 47micro-craters/cm² (Table 2).

AAS 22/5 (4711 km):

Location: 15°06.567'S 78°11.734'E

Eight microtektites have been observed in the SEM from this sample, one of them is a fragment. The remaining 7 microtektites have 190 craters including 9 groove-like craters. The spatial density of micro-impacts reduces to 13/cm² (Table 2) in this sample. There is a marked increase in the percentage of larger craters in this sample (due to a decrease in small craters), starting with the >51µm category and especially those in the >100 and 200 µm categories (Table 3; Fig. 4 b; Fig. 6). The larger craters are invariably shallow, pitless craters, indicating lower collision velocities. This location also marks the beginning of gentle collisions between projectiles and targets.

AAS 22/3 (4889 km)

Location: 16°59.959'S 77°59.792'E

The average size for the 8 microtektites selected for SEM study out of total 27 impacted ones, is 478 µm .The size range of microtektites observed in the SEM is 202-828 µm. In all, these 8 microtektites have recorded 369 impacts including 5 groove-shaped craters. The spatial density of micro-impacts in this sample is 47 micro-craters/cm² . This is an increase over the sample immediately north of this one (AAS 22/5 :4711 km; Table 2, Fig. 7).

Most of the craters are formed due to erosive impacts. Accretionary features are also present in large number. The interesting feature in this sample is that most of the impacts are not showing well formed concentric as well as radial crack-patterns which are indicative of hypervelocity impacts. These craters are mostly small sized depressions on the host in numerous quantities with a central elevated portion and incipient cracks thus indicating comparatively more gentle collisions than the northernmost samples (Fig. 4 f). These pits also appear as closely spaced clusters. Similar clusters have also appeared at 4708 km (AAS38/3,

Fig. 4 d) however based on their geometries (eg. presence of a central pit) it is discernible from Fig. 4, that the projectiles which generated the cluster of micro-impacts on microtektites in AAS38/3 are more numerous and also involved higher velocities. Interestingly, all the impacted microtektites here (AAS22/3 : 4889 km) contain consistently high number of impacts, which is different from the two samples north of this one (i.e., AAS22/5, 4711km; and AAS38/3, 4708 km : Table 2). Some of the impacted microtektites bear scratch marks on their surface. Similar scratch marks have been found quite commonly on lunar surface materials which were interpreted as in-flight low velocity adherents (Carter and MacGregor 1970). This sample also has a high percentage of fragments (~5%).

The pattern of the crater sizes is similar to that of the samples much north of this one (eg. AAS 38/2, 4174 km :Table 3). The collisions however, are much gentler in this sample – the relative encounter velocities seem to be smaller. The above characteristics of the impacts suggest an increase in the number of small projectiles in this sample.

AAS38/4(4843km;4°00.254'S;75°00.070'E) and AAS 62/55 (5008 km; 18°19.480'S;77°55.737'E) :

These two samples have no impacted microtektites.

AAS 62/56 (4969 km):

Location: 18°19.480'S 77°55.737'E

Two samples (AAS38/4 4843 km; and AAS62/55 : 5008 km) have no impacted microtektites. Among all the other samples which show impacted microtektites, this sample has the least number of impacted microtektites in terms of percentage. As mentioned in an earlier section, large quantities of sediment sample were searched at this location for microtektites and out of 2561 microtektites observed only 30 (1.21%) show impact generated features. Out of these, 6 microtektites are observed under the SEM, with all containing only a total of 34 impacts. All craters have large diameters, 58.82% of the crater population is larger than >100 µm diameter

(Table 3; Fig. 6). The spatial density of micro-impacts here (<1 micro-crater/cm²) is the lowest among all observed samples (Table 2, Fig. 7).

Most of the craters are large erosive craters but not of the hypervelocity variety, because the cracks are poorly developed and the craters are invariably shallow (eg. Fig.5 a). Further, large accretionary features are found which are indicative of larger projectile size (Fig. 5b). Thus all the impacts are formed due to comparatively gentle collisions with projectiles having large diameters.

AAS 38/5 (5162 km):

Location: 17°03.194'S 74°02.669'E

This is the southernmost location along the transect and the farthest from the impact site (5162 km). Nine microtektites were selected for SEM study from this sample. These 9 microtektites contain a total of 104 impact generated features. The spatial density of impacts is also very low : 3/cm². A larger percentage of craters (~24 %) fall in the 'large' (>100 μm diameter) category than the samples north of this one (Table 3, Fig. 6).

Most of the impacts seem to be of the gentle variety : large pitless craters (implying collision with larger projectiles) (Fig. 5 c, d, e, f). Some of these craters could also be pit craters with the pit excavated as has been suggested for similar features on lunar surface materials (eg. Hörz et al., 1971). However, the micro-craters in this location have relatively large diameters; if the projectiles that generated these micro-craters had greater impact velocities the host microtektites would have fragmented. And the percent fragments (0.23%) is not high at this site. Also, the accompanying accretionary impacts show welded projectiles (eg. Fig.5 e). All of the above features are indicative of gentle interparticle collisions between ejecta which are generally in quasi plastic state. Only few craters have radial cracks.

The trend here indicates a dissipation of the collisional environment because there are fewer collisions between entrained particles, and most of the impacts indicate lower velocities. Further, the larger sizes of the craters and the sizes of the welded projectiles indicate a larger average size of entrained material. The very small craters as seen in the northern samples (eg. 38/1; 3899 km) are totally absent here.

Results and Discussion

While the parent crater for the Australasian tektite strewn field has not been found yet, all evidence strongly suggest a crater in Indochina (Schnezler et al. 1992; Ma et al. 2004; Glass and Koeberl 2006). The northernmost sample in this study is at a distance of ~3900 km from the proposed impact site in NE Thailand – Central Laos ($12^{\circ}\text{N}; 104^{\circ}\text{E}$: Prasad et al. 2007) and the southernmost location (AAS 38/5) is at a distance of ~5000 km from the same proposed site (Fig. 1). The N-S transect here therefore represents distal ejecta. However, noticeable trends are seen in the micro-craters observed on the microtektite populations along this transect.

There is a general decrease in the average micro-crater diameter with increasing radial distance (Fig.7). The smaller sized craters are dominant in the northern parts of the transect, and this trend is reversed in the southern part with increasing radial range. It is seen that the morphology and types of micro-impacts change systematically with radial range. The micro-impacts in AAS38/1 (3899 km) are mostly of the hypervelocity type (it is again emphasized here, that this term is used to gauge craters which have recorded relatively higher projectile velocities) with central, glass-lined pits, surrounded by radial and concentric fractures; these surfaces also contain very few accretionary impacts (Fig. 2a,b). Towards the South (e.g. AAS 62/56; 5008 km) the collisions are more gentle and the impactors increase in size. (Fig. 2 g, h; Figs. 6,7). The alternative explanation for this trend could be that the microtektites from the three southernmost samples in the transect could have experienced greater etching which could have effectively obliterated micro-craters in the smaller size ranges. The only sample which forms a minor discordant note in both the above trends (spatial density and crater size) is AAS 22/3 (4889 km). Here the dominant range of crater diameters is $< 50 \mu\text{m}$, with a sizeable population in the range 11-25 μm (Table 2, Fig. 6). However, the type of impacts here is interesting. These are mostly 'soft' collisions where the projectiles have made shallow impacts without generating radial and concentric cracks. The collisional energies between particles at this distal end of the transect therefore are very low.

Spatial density of micro-impacts : spatial density of micro-impacts or number of micro-craters on the surfaces of microtektite/cm² of the ocean floor at a given location is employed here to indicate intensity of interparticle collisions. There is a definite decrease in the spatial density from with increasing distance from the source crater (Fig. 7). This is accompanied by a general decrease in the microtektite abundance (no. of microtektites of >125 μm diameter/cm² : Table 1), an increase in average microtektite diameter and an increase in the micro-crater diameter with distance from the proposed source crater location (Fig. 7).

The above trend is also accompanied by variations in the size and type of the micro-craters. Tables 1,2,3 and Figs.6,7 reveal the two extrema in 38/1 and 62/56 with regards to the size of the micro-craters along the transect, with fluctuations in the locations in between. It is discernible that a majority of the micro-crater population (73 %) resides in the <25 μm diameter in AAS38/1, whereas no single microimpact of <25 μm diameter was found in AAS 62/56, and the dominant crater population (58%) in this most distant sample is >100 μm. The number of micro-craters indicates the number of projectiles, which should decrease away from the source crater as the abundance decreases. The more distal ejecta enters the atmosphere at a shallower angle. The finer ejecta, that produce the smaller craters, are decelerated faster than the larger microtektites.

Timing of collisions: Vickery (1986) and Melosh (1989) suggested that during the excavation stage of a major impact, an ejecta cloud first leaves the impact site which is closely followed by a faster moving vapor cloud. There would be violent interactions between these two clouds which would result in the decimation of the ejecta cloud (Vickery 1986). We had suggested earlier that this could be a plausible scenario for the occurrence of collisions between particles leading to the micro-impact phenomena (this would take place before the microtektites left the atmosphere). However, considering the larger geographic control on the data along a transect, the following scenario emerges :

Firstly, If ALL the collisions are indeed the products of the collisions between the ejecta and vapor plumes (implying they are all collisionally processed at the at same time and location and under similar conditions), then there should not be substantial differences between the characteristics of the micro-craters as one moves radially away from the impact source area. All the impacted microtektites should have more or less the same or similar numbers of micro-

craters and also the intensity i.e., all microtektites should register largely similar types of craters. However, this is not so. We find the northern parts of the transect showing larger number of microimpact craters which are indicative of relatively greater velocities, larger number of smaller craters and a larger percentage of microtektites are affected by collisional activity and greater percentage of fragments. The trend is almost the opposite in the southernmost samples of the transect studied here (Figs 6 & 7).

Nearer to the crater, volumes of the ejecta would be largest in number, therefore the forward motion of the ejecta would lead to greater chances of violent collisions. The intensity of the collisional activity should thus decrease with increasing distance from the source crater because of the reduction in the numbers of entrained particles with distance. The microtektite abundance nearer to the source crater for the Australasian tektite strewn field is the highest, in the orders of several thousands of microtektites/cm² (9834 microtektites/cm² in ODP 1144A : Glass and Koeberl 2006). Further, the data presented by Glass et al. (1997), and Glass and Koeberl (2006) also shows a much higher percentage of fragments nearer to Indochina region, the maximum being 75 % in sample number ODP 1144A which is located 20.05°N latitude and 117.42° E longitude close to the Indochina region at a distance of 1412 km from the source crater proposed by Glass and Koeberl (2006). Compare this with 1.59 % fragments, and 86 microtektites/cm² abundance in the northernmost sample in the transect observed here (3899 km : AAS38/1). If fragments are indeed indicative of catastrophic collisions between entrained particles (we have observed in this study as well as in our earlier studies, eg. Prasad and Sudhakar, 1998; Prasad et al., 2003, that many fragments bear the evidence that they were broken by collisional activity), then it is not surprising that a large percentage of the microtektites found nearer to the source crater turn out to be fragments, and “some of the microtektites from Hole 1144A have obvious impact pits on their surfaces” (Glass and Koeberl 2006).

Atmospheric interaction would have the tendency to suddenly bring together particles which have been otherwise travelling at steady velocities due to aero-braking, this in effect provides an environment where collisions could take place. The microimpact feature observed on the anterior side of Central Indian Ocean tektite (a flanged australite button) (Glass et al. 1996) is a strong indicator of this phenomenon. Several tektites in Australia commonly show

aerodynamic phenomenon in the form of a development of a flange which is the pull-back material of surface melt of a tektite formed during the descent resulting in a button shape (O'Keefe 1976). The anterior and the posterior sides of these tektites are quite distinct and large number of studies have been made on this aspect (see refs. in O'Keefe 1976). A similar flanged australite button was discovered in the Central Indian Ocean (Fig.1) (Prasad and Rao 1990), the anterior portion of this tektite contains a distinct microimpact feature (Glass et al. 1996). Quite obviously, the microimpact on the anterior has taken place only **after** the formation of the flange and most definitely during the descent of the tektite. This micro-impact therefore gives a more definitive evidence for the geographical placement of the collisional phenomena.

Furthermore, Folco et al. (2009) observed 465 Australasian microtektites from Transantarctic mountain which is roughly 9000 km away from the source region in Indochina, they reported the absence of micro-impact phenomena on the surfaces of these microtektites. Therefore, beyond a certain distance from the source crater interparticle contact between the ejecta would be reduced completely and collisional activity ceases.

Possible planetological relevance :

Martian Ejecta : It has been predicted that the polar regions of Mars should contain well preserved layers of distal ejecta (Wrobel and Schultz, 2004), where micro-impact features on the ejecta would provide key evidence for their identification as distal ejecta (Lorenz 2000). It would be interesting to see the morphology of the micro-impact features on the ejecta, as they could provide important clues to the proximity of the impact craters.

Venusian ejecta parabolas: Schaller and Melosh (1998) studied 57 impact craters and their ejecta on Venus. They observed that the ejecta is deposited in parabolas which form annular rings of increasingly larger diameters with increasing distance from the source crater and these parabolas are the result of atmospheric interaction with the entrained ejecta. They proposed that the particles that define these parabolas are usually of comparable sizes and they

decrease in size with increasing distance from the impact site – a close parallel to this phenomenon on earth they observed would the distribution of ejecta from the Chicxulub and distribution of tektite and microtektite strewn fields on earth. In view of the above observations, there appears a possibility of observing interparticle collisional activity on Venusian ejecta as well.

Conclusions

From the observation of 4110 microimpact phenomena identified by extensive examination of Australasian microtektites from 11 sediment cores along a roughly N-S transect in the central Indian Ocean spanning over 1300 km in radial range from a suggested parent crater location (between $04^{\circ} 58.564'S$ & $78^{\circ} 01.204'E$ and $17^{\circ} 57.223'S$ & $78^{\circ} 01.711'E$) the following conclusions emerge: Although all the samples studied here would fall under the distal ejecta regime, distinct trends are observed with geographic distances from the proposed location of the source crater NE Thailand – Central Laos ($12^{\circ}N;104^{\circ}E$: Prasad et al. 2007). Average microtektite size increases and average micro-crater size increase with distance from proposed source crater location. Particle to particle impacts were more gentle away from the source. The fraction of impacted microtektites and the spatial density of micro-craters decreases away from the source crater. These parameters indicate decreasing collisional activity with decrease in ejecta concentration radially away from the source crater. The micro-craters closer to the source crater are small in diameter and correspond to hypervelocity collisions, but farther from the source crater the collisions were gentle (represented by pitless craters and depressions), and by relatively large particles (the micro-crater diameter is large). The above observation implies more dense ejecta with larger numbers of small particles in flight closer to the source crater. Divergence of ejecta downrange, results in decreasing interparticle contact. These trends can be extrapolated closer to the impact site, where a very high percentage of fragments (implying destructive collisions) and abundance (implying density of ejecta) were recorded in earlier studies (Glass and Koeberl, 2006). Also, at the most distal parts of the ejecta, there would be no interparticle contact and therefore zero

collisional activity. Therefore, this study shows that there is a systematic difference in the morphology and numbers of the micro-impact phenomena in the radial range of ejecta from large scale, oblique impacts.

The collisional activity seems to take place during the descent of the ejecta particles especially as a result of atmospheric interaction with the ejecta. The micro-crater on the anterior part of the Central Indian Ocean flanged button offers a clear proof of this.

This study further hints at the possibility of interparticle collisional activity in the ejecta of Mars and Venus as well.

Acknowledgements

The authors are grateful to Director, NIO for providing the facilities and the encouragement for carrying out this work. The sample have been collected in many cruises and several colleagues have been helpful in sediment sampling onboard, and project assistants over the years in processing - we express our gratitude to all who helped in this endeavor. We are extremely grateful for the thought provoking, incisive reviews by an anonymous reviewer and Ralph D. Lorenz, University of Arizona which helped improve the manuscript substantially. We are also grateful to Friedrich Hörz of NASA, Johnson Space Center and Natalia Artemieva, Institute for Dynamics of Geospheres, Moscow, for their invaluable suggestions, criticisms on an earlier version of this manuscript which helped us to improve considerably. The authors are also grateful to Vijay Khedekar and Areef Sardar for the help in the SEM work. This research has made use of NASA's Astrophysics Data System. This is NIO's contribution no.....

REFERENCES

- Artemieva N.A. 2002. Tektite production in oblique impacts. 32nd Lunar and Planetary Science Conference, abstract # 1216.
- Carter J.L., and Macgregor I.D. 1970. Mineralogy, petrology and surface features of some Apollo 11 samples. Proceedings Apollo 11 Lunar Science Conference, *Geochimica et Cosmochimica Acta Supplement 1*, 247-265.
- Christiansen E.L. 1993. Design and performance equations for advanced meteoroid and debris shields. *International Journal of Impact Engineering* 14, 145-156.
- Folco L., D’Orazio M., Tiepolo M., Tonarini S., Ottolini L., Perchiazzi N., Rochette P., and Glass B.P. 2009. Transantarctic Mountain microtektites : Geochemical affinity with Australasian microtektites. *Geochimica et Cosmochimica Acta* 73, 3694 – 3722.
- Gault D.E., and Wedekind J.A., 1978. Experimental studies of oblique impact. Proceedings Lunar Planetary Science Conference IX, 3843-3875.
- Glass B.P. 1990. Tektites and microtektites : Key facts and inferences. *Tectonophysics* 171, 393-404.
- Glass B.P., and Koeberl C. 2006. Australasian microtektites and associated impact ejecta in the South China Sea and the Middle Pleistocene supereruption of Toba. *Meteoritics and Planetary Science* 41, 305-326.
- Glass B.P., and Pizzuto J.E. 1994. Geographic variation in Australasian microtektites concentrations: Implications concerning the location and size of source crater. *Journal of Geophysical Research* 99, 19,075 – 19,081.
- Glass B.P., and Wu J. 1993. Coesite and shocked quartz discovered in the Australasian and North American microtektite layers. *Geology* 21, 435-438.
- Glass B.P., Chapman D.R., and Prasad M.S. 1996. Ablated tektite from the Central Indian Ocean. *Meteoritics and Planetary Science* 31, 365-369.
- Glass B.P., Muenow D.W., Bohor B.F., and Meeker G.P. 1997. Fragmentation and hydration of tektites and microtektites. *Meteoritics and Planetary Science* 32, 333-341.
- Glass B.P., Swincki M.B., and Zwart P.A. 1979. Australasian, Ivory Coast and North American tektite strewn fields: Size, mass, and correlation with geomagnetic reversals and other earth events. Proceedings 10th Lunar Science Conference, 2535-2545.

Hörz F., Hartung J.B., and Gault, D.E. 1971. Micrometeorite craters on lunar rock surfaces. *Journal of Geophysical research* 76, 5770-5798.

Hutcheon I.D. 1975. Micrometeorites and solar flare particles in and out of the ecliptic. *Journal of Geophysical Research* 80, 4471-4483.

Koeberl C. 1994. Tektite origin by hypervelocity asteroidal or cometary impact : Target rocks, source craters, and mechanisms. In *Large meteorite impacts and planetary evolution*, Edited by Dressler B.O., Grieve R.A.F., and Sharpton V.L. Special Paper The Geological Society of America, 293, Boulder. Pp 131-151

Kunz J., Bollinger K., Jessberger E.K., and Storzer D. 1995. Ages of Australasian tektites . Lunar and Planetary Science Conference XXV,. 809-810. (abstract).

Lorenz R.D. 2000. Microtektites on Mars : Volume and texture of distal impact ejecta deposits. *Icarus* 144, 353-366.

Ma P., Aggrey K., Tonzola C., Schnabel C., de Nicola P., Herzog G.F., Wasson J.T., Glass B.P., Brown L., Tera F., Middleton R., and Klein J. 2004. Beryllium-10 in Australasian tektites : Location of the source crater. *Geochimica et Cosmochimica Acta* 68, 3883-3896.

Melosh H.J., 1989. Impact cratering, a geologic process. Oxford Univ. Press, New York, USA. 245 pp.

O'Keefe J.A., 1976. Tektites and their origin. Elsevier, Amsterdam. 254 pp

Pierazzo E., and Melosh H.J. 2000a. Understanding oblique impacts from experiments, observations, and modeling. *Annual Reviews Earth and Planetary Sciences* 28, 141-167.

Pierazzo E., Melosh H.J. 2000b. Melt production in oblique impacts. *Icarus* 145, 252-261.

Prasad M.S., and Rao, P.S. 1990. Tektites far and wide. *Nature* 347, 340.

Prasad M.S., and Sudhakar M. 1996. Impact microcraters on an Australasian microtektite. *Meteoritics and Planetary Science* 31, 46-49.

Prasad M.S., and Sudhakar M. 1998. Microimpact phenomenon on Australasian microtektite: Implications for ejecta plume characteristics and Lunar surface processes. *Meteoritics and Planetary Science* 33, 1271-1279.

Prasad M.S., and Khedekar V.D. 2003. Impact microcrater morphology on Australasian microtektites. *Meteoritics and Planetary Science* 38, 1351-1357.

- Prasad M.S., Mahale V.P., and Kodagali V.N. 2007. New sites of Australasian microtektites in the Central Indian Ocean: Implications for the location and size of source crater. *Journal of Geophysical Research*, 112, E06007, doi: 10.1029/2006JEO00857, 2007.
- Schaller C.J., and Melosh H.J. 1998. Venusian ejecta parabolas : Comparing theory with observations. *Icarus* 131, 123-137.
- Schnetzler C.C., Walter L.S., and Marsh J.G. 1992. Mechanism of Mong Nong-type tektite formation and speculation on the source of Australasian tektites. *Meteoritics* 27, 154-165.
- Schultz P.H. 1996. Effect of impact angle on vaporization. *Journal of Geophysical Research* 101, 21117-21136.
- Schultz P.H. 1999. Ejecta distribution from oblique impacts into particulate targets. 28th Lunar and Planetary Science Conference, abstract, 1259-1260.
- Schultz P.H., and D'Hondt S. 1996. Cretaceous-Tertiary (Chicxulub) impact angle and its consequences. *Geology* 24, 963-967.
- Stoffler D., Artemieva N.A., and Pierazzo E. 2002. Modeling the Ries-steinheim impact event and the formation of the moldavite strewn field. *Meteoritics and Planetary Science* 37, 1893-1907.
- Vickery A.M. 1986. Effect of an impact-generated gas cloud on the acceleration of solid ejecta. *Journal of Geophysical Research* 91, 14139-14160.
- Wrobel K.E., and Schultz P.H. 2004. Effect of planetary rotation on distal tektite deposition on Mars. *Journal of Geophysical Research* 109, E05005, doi: 10.1029/2004JE002250, 2004.

FIGURE LEGENDS :

FIGURE 1 : Map showing the Australasian tektite strewn field, the boundaries of the strewn field as per Folco et al. (2009). The stars in the Central Indian Ocean form the transect of samples in this study. The square shape in Indochina (1) ($22^{\circ}\text{N};104^{\circ}\text{E}$) is the proposed location of source crater by Glass and Koeberl (2006); the pentagon shape (2) ($12^{\circ}\text{N}; 106^{\circ}\text{E}$) is the probable location of the source crater proposed by Prasad et al. (2007). Filled circles close to the proposed source crater are microtektite sites which have very large microtektite abundances, and a high percentage of fragments (up to 74%) : data from Glass and Koeberl (2006). Dashed line represents the proposed boundaries of the strewn field (Glass and Wu 1993) and the hatched portion in Australia is the area where aerodynamically ablated Australasian tektites have been found.

Figures 2-5 depict SEM images of typical micro-impacts registered on microtektites along the N-S transect

FIGURE 2 : Micro-impact features in the northernmost sample AAS 38/1 (3899km distance from the postulated source crater).

A : Microtektite showing numerous small impacts on its surface along with few larger ones that contain a central pit and radial cracks (P2 in Table 2).

B: A part of the above microtektite under high magnification. Clusters of closely spaced micro-craters showing sand blasting of the microtektite surface, all of relatively similar sizes which gives an indication of the projectile dimensions available at this distance. Many of the micro-craters possess central pit, radial and concentric cracks which are indicative of relatively greater velocities.

C: One 'high velocity' crater under high magnification from this location. Note the central depressed pit, radial and concentric cracks (P3 in Table 1).

D: An accretionary "pancake" on a microtektite from the same location (38/1, P7 in Table 2).

E : Another accretionary pancake feature from AAS 38/2 (P6) a low velocity impact of the projectile while it was still in a plastic state.

F : Large shallow, pitless crater from the northernmost sample (AAS 38/1, P7) seen on a microtektite.

FIGURE 3 : Micro-impact features seen on samples at distances between 4052 km (AAS 22/8) and 4284 km (AAS 22/7) from the suggested source crater

A : Welded projectile on a microtektite representing extremely gentle impact (AAS22/8, P1)

B: A fragmented microtektite (inset), fragmentation because of micro-impact producing collision – evidence for micro-cratering seen on exposed ‘surface’ of the microtektite (AAS22/8, P9).

C: A disc-shaped microtektite showing few low velocity impacts in terms of welded projectiles (AAS38/2, P1).

D: Large pitless crater on a microtektite (AAS38/2, P3)

E: Low angle oblique impact on AAS38/2, P7 which produced a groove-like crater. This disc-shaped microtektite has accumulated 304 such micro-impacts.

F : Sub-micrometer impacts on AAS22/7, P4, these craters bear resemblance to those observed on Apollo 17 rocks (Hutcheon 1975)

FIGURE 4 : Micro-impact features on samples at distances between 4284 km (AAS22/7) and 4889 km (AAS22/3) from the suggested source crater in Indochina.

A: A broken microtektite from AAS22/7 (P6), fragmented by a micro-impact

B : Large shallow, pitless craters on a microtektite (AAS22/5, P3), indicative of lower collisional velocities than implied by craters having a central pit, prominent radial and concentric cracks

C : A microtektite from AAS38/3 (P6) sandblasted by small projectiles, registering >400 micro-impacts – the highest number observed in the present study. Note that most of the impacts have a central glass-lined pit and presence of few radial cracks. See “D” for a close up view of this microtektite.

D : A portion of the microtektite shown in “C” showing the close-spaced cluster of micro-impacts. Note that most of the impacts have a central glass-lined pit and presence of few radial cracks.

E : Microtektite in the southern part of the transect (4889 km, AAS22/3, P2) showing a large pitless crater with multiple radial cracks. The impact seems to have excavated a portion of the microtektite. This microtektite also contains numerous very small micro-impacts on its surface a portion of which is shown in “F”

F: A portion of microtektite seen in “E” above showing ‘soft’ collisions of projectiles with relative lower collisional velocities as compared with “D” above. The impacts here seem to have produced small depressions but with few radial or prominent concentric cracks.

FIGURE 5 : Micro-cratering in the southernmost part of the transect between distances of 4969 km (AAS 62/56) to 5162 km (AAS38/5)

A: Large sized microtektite (AAS62/56, P2) with large diameter, shallow impact craters – very few impacts on each microtektite are recorded in this part of the transect

B: Low velocity impact with welded projectile on a large sized microtektite (AAS62/56, P6)

C: Low velocity impacts on a microtektite in the southernmost sample (AAS38/5) with few incipient cracks and a small excavated portion of the host microtektite are discernible.

D : Two impact craters seen on “C” above under higher magnification

E: Large sized microtektite showing few impacts which are large in dimensions, delivered under low velocity conditions - welded projectiles are visible

F: Shallow, large, pitless crater and low velocity welded projectile observed in the southernmost sample (AAS38/5; 5162 km).

FIGURE 6 : Spatial density of micro-impacts (i.e., the number of micro-craters on microtektites per 1 cm² of the ocean floor), which shows the numbers of micro-craters of different sizes with increasing distance from the source region. While the northern part of the transect contains large numbers of craters of all sizes compared with the southern part, the micro-impacts with smaller diameters (<50 µm) dominate the micro-crater population in the north. Although the absolute numbers of the micro-craters with the larger diameters (especially >200 µm) may show a more gentle decrease towards the south, however percentage-wise there is a strong increase in the percentage of micro-craters with large diameters and very few craters with smaller diameters (<50 µm) in the southern part of the transect (please see Table 3).

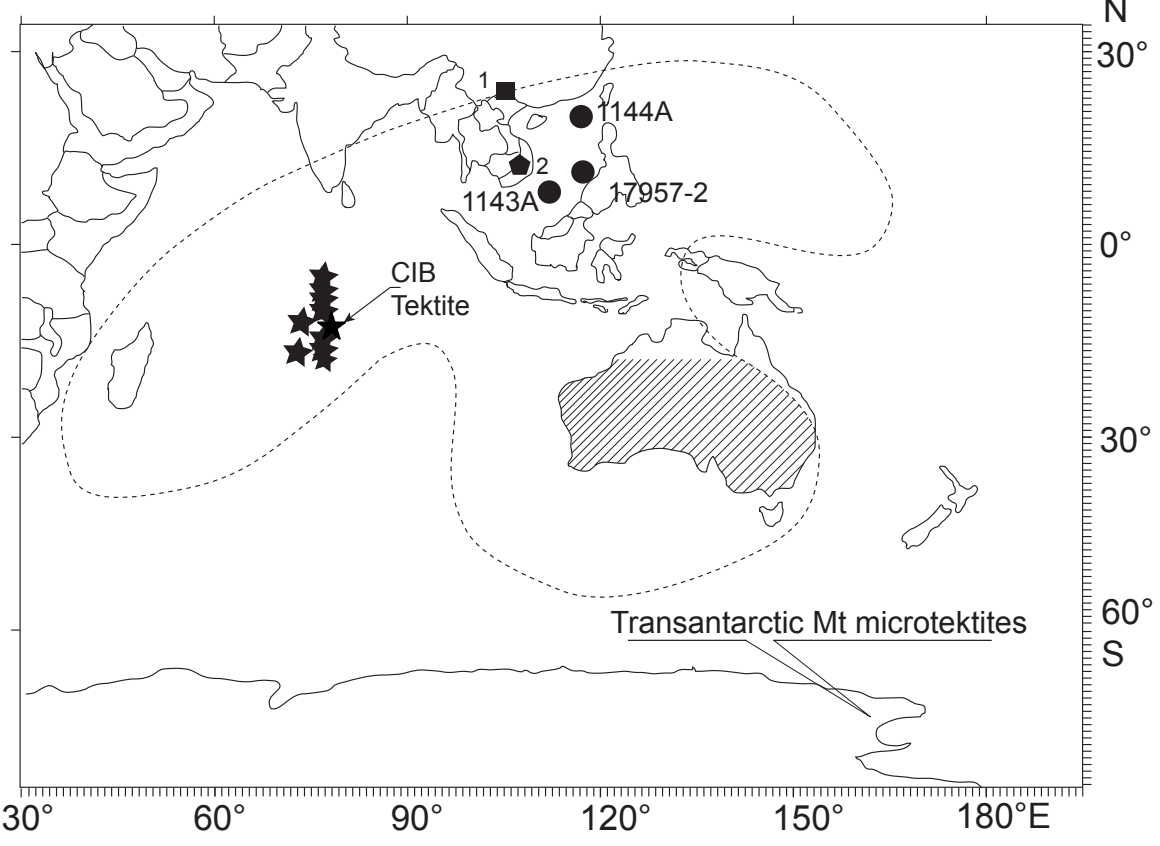
FIGURE 7 : Variation in different parameters with increasing radial distance from the suggested source crater (12⁰N; 106⁰E) for the Australasian tektite strewn field. Triangles show average values, the envelope at each site shows the range in which 50% of the values occur.

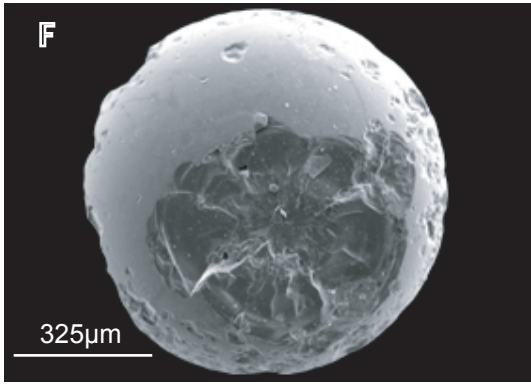
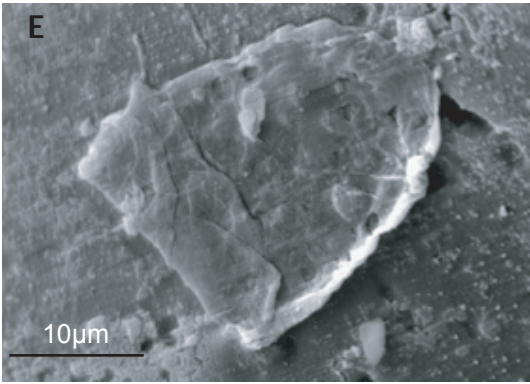
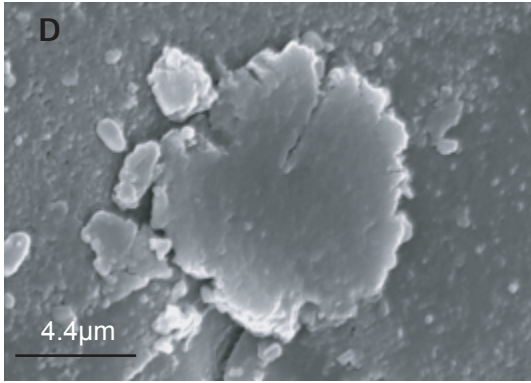
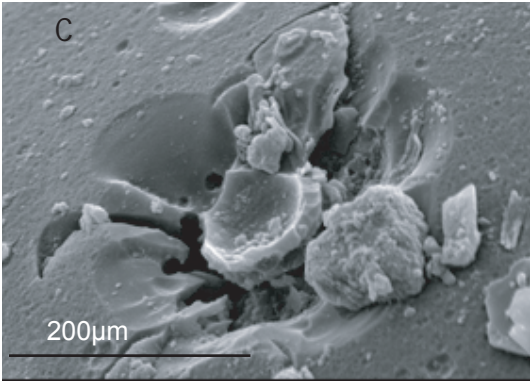
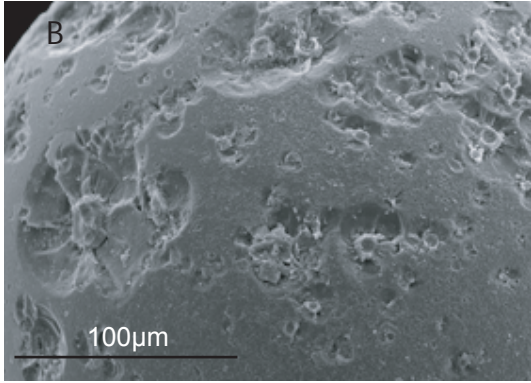
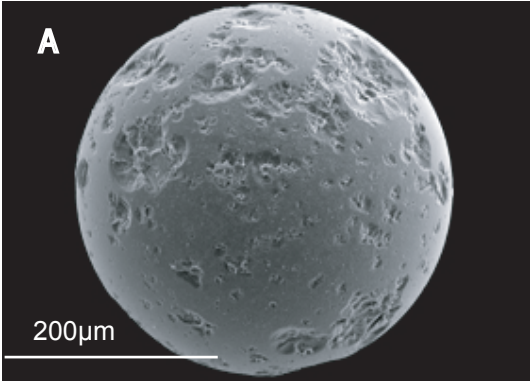
LEGENDS TO TABLES

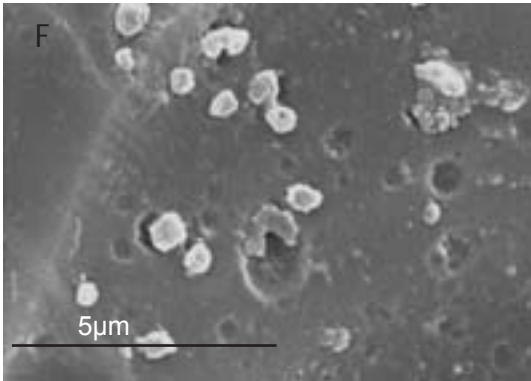
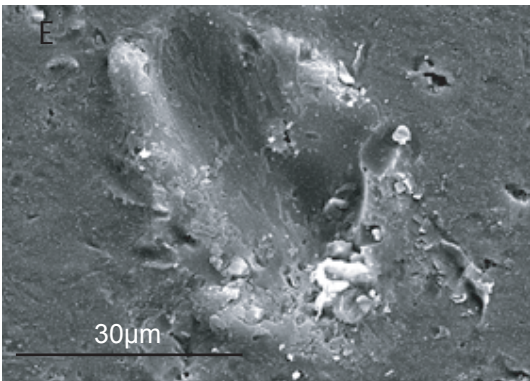
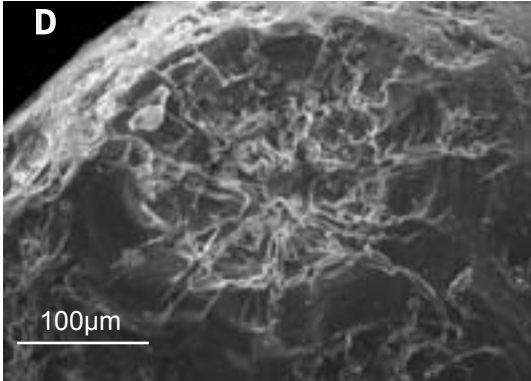
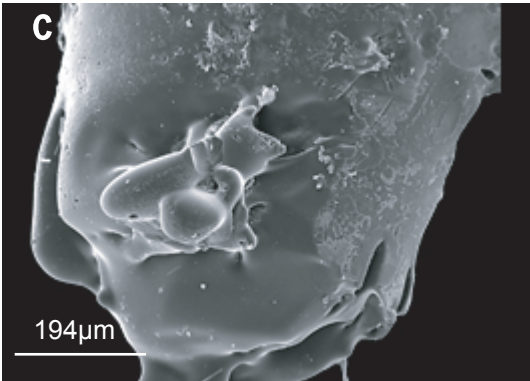
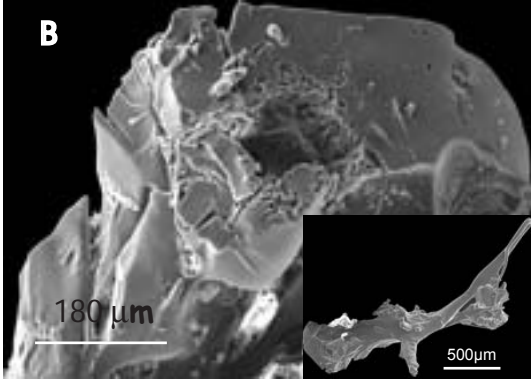
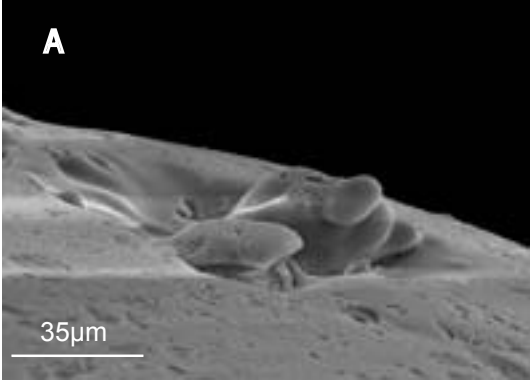
Table 1 : Overview of micro-impacts from the samples along the transect

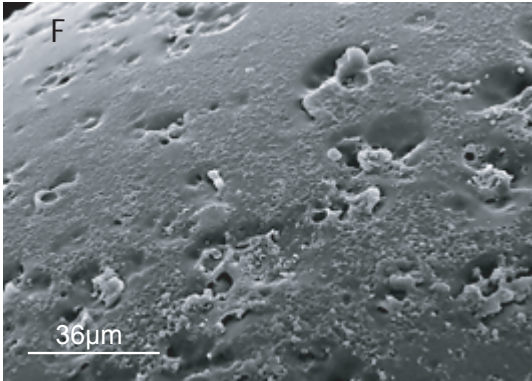
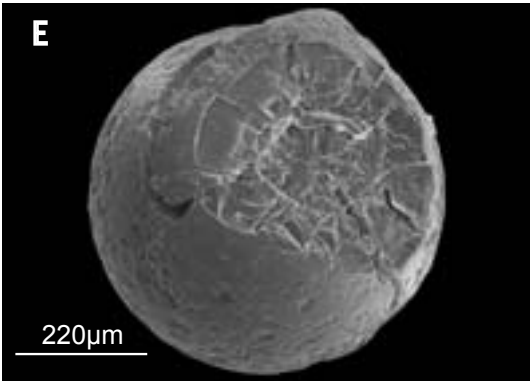
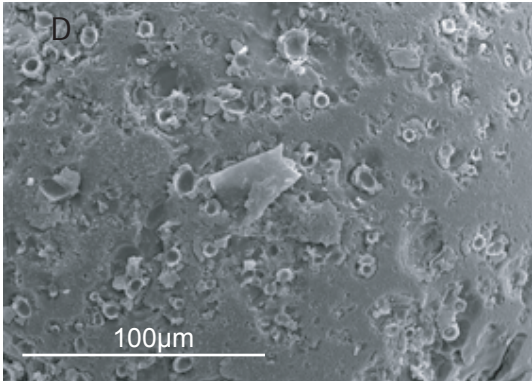
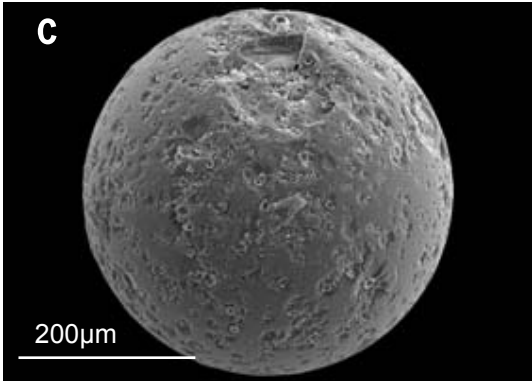
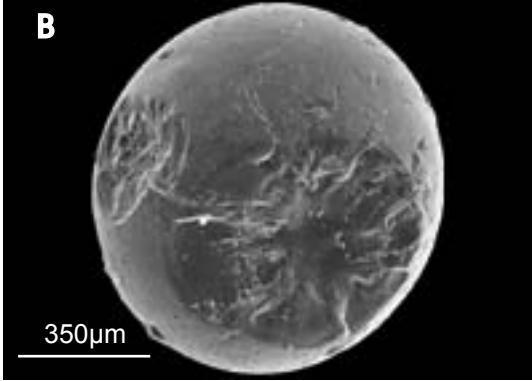
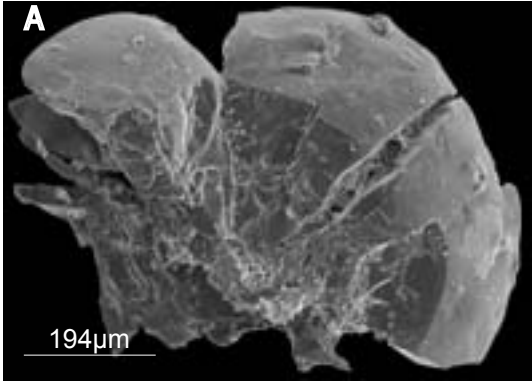
Table 2 : Number of impact generated features on individual microtektites from each of the samples along the transect as observed in the SEM

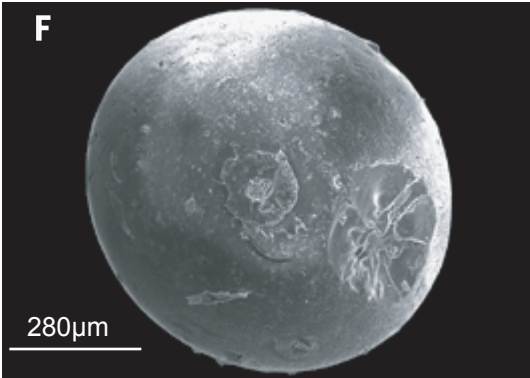
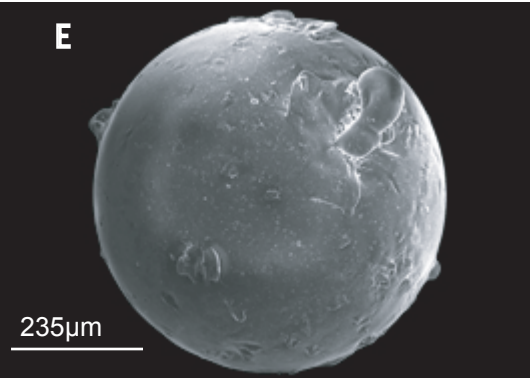
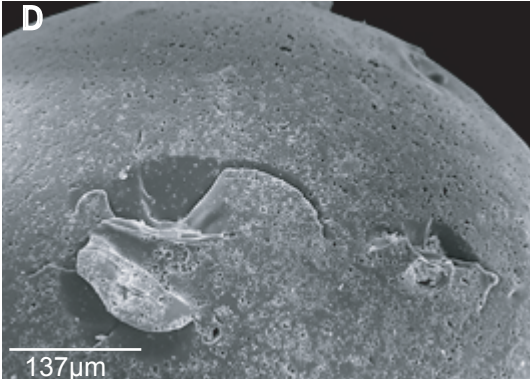
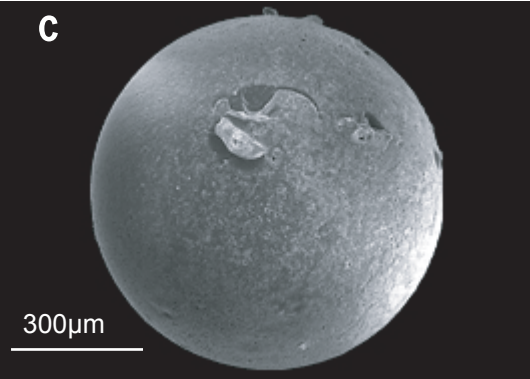
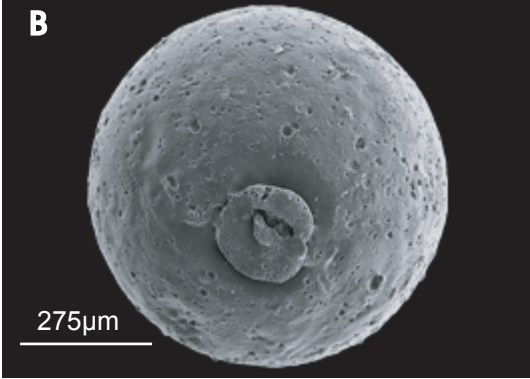
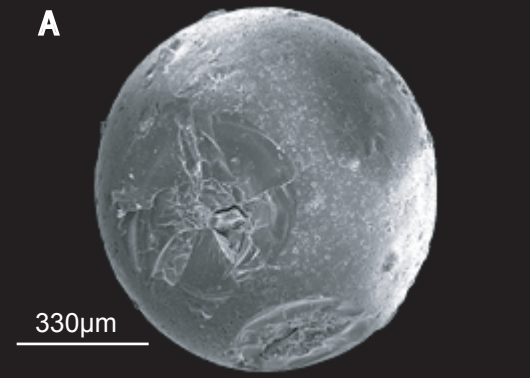
Table 3 : Number of impacts in different size ranges/cm² in the samples along the transect.











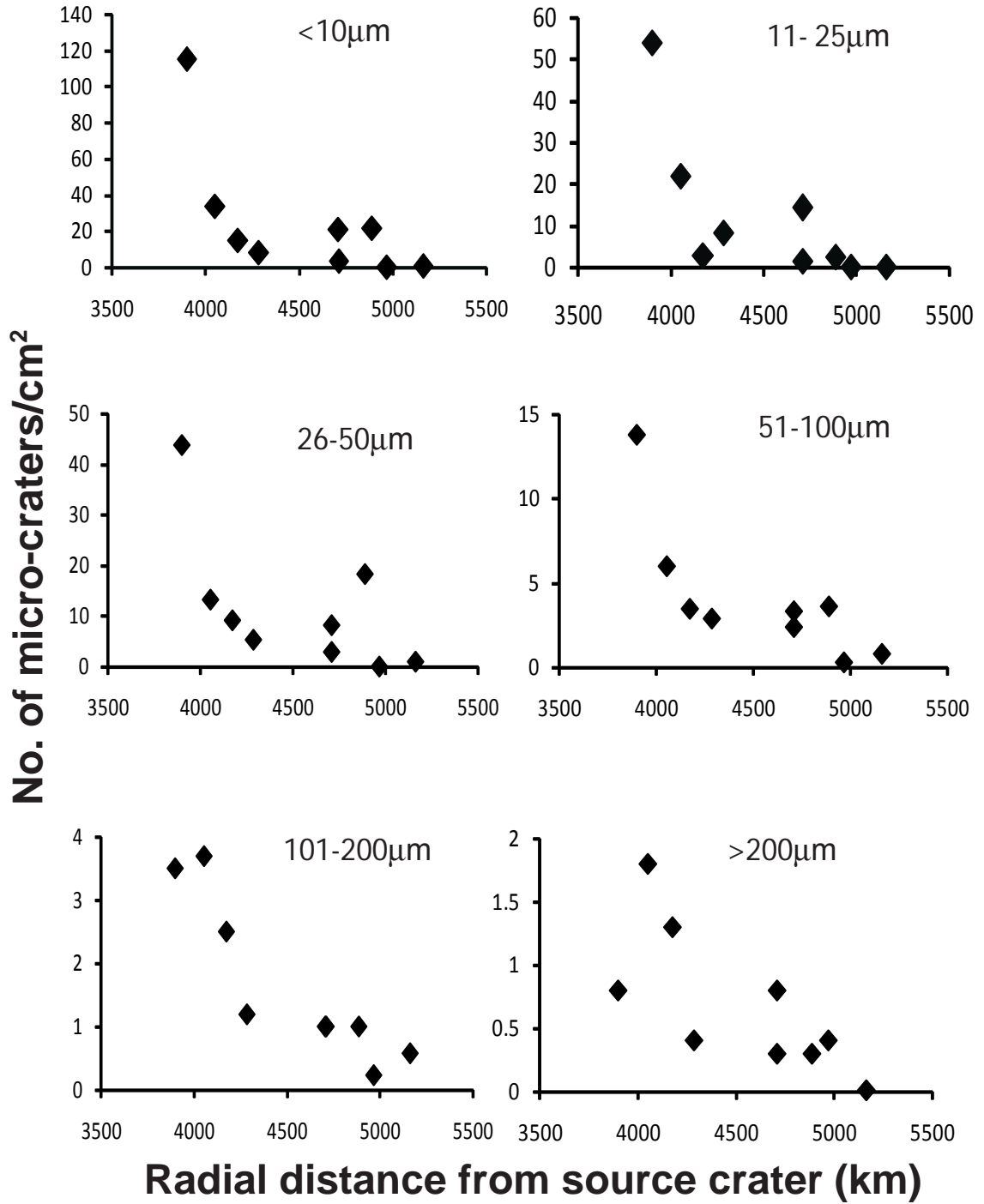


Table 1: Overview of micro-craters from the samples along the transect

Sample No.	Location	Water Depth (m) and Sediment type	Distance from source crater* (km)	Abundance of >125µm size microtektites/cm ² *	Average microtektite diameter (µm)*	Total microtektites observed (>250 µm diameter)	% of impacted microtektites	% of fragments	Size range of impacted microtektites (µm)	Average size of impacted microtektites (µm)	No. of microtektites observed in SEM
AAS38/1	04°58.564'S 78°01.204'E	4560 Sil. ooze	3899	86	250 ± 97 (n=104)	503	7.95	1.59	275-911	428 ± 169	12
AAS22/8	07°05.289'S 78°07.712'E	5180 Sil.ooze	4052	91.3	259 ± 98 (n=155)	323	7.73	6.81	345-1026	612 ± 299	7
AAS38/2	8°29.868'S 77°59.761'E	5438 Sil.ooze	4174	30.0	257 ± 99 (n=168)	139	14.38	2.15	647-1530	1002 ± 427	7
AAS22/7	10°00.988'S 78°08.971'E	5260 Sil.ooze	4284	50.1	263 ± 104 (n=92)	255	7.45	5.49	414-1112	764 ± 199	5
AAS38/3	12°34.831'S 75°15.351'E	5320 Sil.ooze	4708	21.0	285 ± 179 (n=149)	115	13.04	0	430-1000	626 ± 209	7
AAS22/5	15°06.567'S 78°11.734'E	5000 Sil.ooze	4711	33.9	353 ± 250 (n=56)	193	7.25	4.66	418-1284	795 ± 418	7
AAS38/4	14°00.254'S 75°00.070'E	4935 Sil. ooze	4843	2.2	244 ± 112 (n=6)	18	0	0	n/a	n/a	0
AAS22/3	16°59.959'S 77°59.792'E	4760 Sil.ooze	4889	21.8	314 ± 155 (n=70)	215	12.55	5.11	202-828	485 ± 257	8
AAS62/56	17°57.223'S 78°01.711'E	4740 Red clay	4969	5	289 ± 158 (n=49)	2561	1.21	0.23	500-978	744 ± 169	6
AAS62/55	18°19.480'S 77°55.737'E	4800 Red clay	5008	<1	393 ± 168 (n=9)	153	0	0	n/a	n/a	0
AAS38/5	17°03.194'S 74°02.669'E	4850 Red clay	5162	8.2	320 ± 216 (n=74)	129	17.82	3.87	503-847	700 ± 108	9
	TOTAL					4604					68

*The average diameters are for microtektites >125 µm in diameter

Table 2 : Number of impact generated features on individual microtektites from the samples along the transect as observed in the SEM.

Sample No.	Number of micro-craters on individual microtektites / diameter of microtektite (μm)												Total no. of impacts	Spatial density of micro-craters (No. of micro-craters on the surface of microtektites / cm^2 of the ocean floor at each site)
	P1	P2	P3	P4	P5	P6	P7	P8	P9	P10	P11	P12		
AAS 38/1	39/ 275	136/ 365	145/ 487	59/ 304	148/ 508	149/ 400	34/ 902	81/ 358	126/ 453	105/ 377	96/ 281	69/ 414	1171	230
AAS 22/8	38/ 1026	17/ 963	26/ 772	74/ 345	20/ 445	58/ 364	222/ 373						452	80
AAS 38/2	29/ 1530	99/ 688	128/ 662	275/ 647	7/ 1064	27/ 1530	304/ 895						869	34
AAS 22/7	11/ 1014	5/ 1113	58/ 552	201/ 414	18/ 729								293	26
AAS 38/3	16/ 512	65/ 1000	8/ 707	14/ 431	23/ 742	441/ 401	42/ 594						609	47
AAS 22/5	35/ 589	13/ 880	8/ 970	58/ 419	17/ 735	10/ 1284	49/ 692						190	13
AAS 22/3	78/ 479	87/ 614	14/ 828	28/ 515	11/ 257	32/ 205	89/ 666	30/ 318					369	47
AAS 38/4	No impacted microtektites in this sample													Nil
AAS 62/56	9/ 978	9/ 880	7/ 501	4/ 642	3/ 720	2/ 746							34	<1
AAS62/55	No impacted microtektites in this sample													Nil
AAS 38/5	2/ 847	4/ 705	14/ 658	4/ 834	23/ 503	2/ 692	25/ 725	3/ 759	27/ 590				104	3
Total number of micro-craters observed												4091		

Table 3 : No. of micro-craters of different sizes on the surface of microtektites / cm² of the ocean floor at each site

Sample No.	<10 μm	11-25 μm	26-50 μm	51-100 μm	101-200 μm	>200 μm
AAS38/1	54.0	115	43.7	13.8	3.5	0.8
AAS22/8	21.8	33.6	13.2	6	3.7	1.8
AAS38/2	2.8	14.8	9.1	3.5	2.5	1.3
AAS22/7	8.3	8	5.2	2.9	1.2	0.4
AAS38/3	14.2	20.8	8.3	2.4	1	0.3
AAS22/5	1.4	3.4	2.9	3.3	1	0.8
AAS22/3	2.5	21.3	18.3	3.6	1	0.3
AAS62/56	0	0	0.08	0.3	0.2	0.4
AAS38/5	0.05	0.5	0.9	0.8	0.6	0.01